POLYNOMIAL MATRIX APPROACH TO INDEPENDENT COMPONENT ANALYSIS: (PART II) APPLICATION

Kenji Sugimoto * **Arata Suzuki** ** **Masuhiro Nitta** *
Naotoshi Adachi *

* *Graduate School of Information Science, Nara Institute of Science and Technology, Nara, 630-0192, JAPAN*
** *Nara Institute of Science and Technology, and ZOJIRUSHI Corporation, JAPAN*

Abstract: This paper proposes two types of application of the method given in the paper (PART I). The first is suppression of disturbance with unknown dynamics in control systems. Assuming that a disturbance enters into a system independently of the control input signals, the method makes it possible to identify a denominator polynomial matrix of the disturbance dynamics, and then to design an H_∞ controller suppressing the effect of the disturbance. Numerical simulation is carried out to verify the effectiveness of this approach. The second is fault detection of mechanical systems subject to vibration from the environment. The vibration source is assumed to be unmeasurable, and yet the method achieves detection of a parameter change of the system due to fault. To test the effectiveness of the second approach, experiment with a flexible structure has been carried out.

Keywords: independent component analysis, disturbance suppression, fault detection, application of polynomial system analysis

1. INTRODUCTION

In our companion paper (Sugimoto and Nitta, 2005), which is presented also in this conference, we have seen that polynomial matrix fraction is effective for independent component analysis (ICA) for a class of dynamical systems, and thereby derived a method for blind identification; i.e., system identification where input signals are not available. The objective of the present paper is to provide two types of application of the method proposed in (Sugimoto and Nitta, 2005).

[1] This work is supported in part by Scientific Research Grant-in-Aid 15560379 from the Japan Society for the Promotion of Science.

In system identification, it is usually natural to expect that the input signal is measurable, because our main objective is to design the control input after we have identified the system parameter (Ljung, 1987). This is, however, not always the case in practice. For example, if the input is subject to nonlinearity, then we are uncertain whether or not we are applying a correct (designed) signal to the input. In this paper, we propose yet a couple of other applications where an input signal is unknown and we need to estimate the dynamics corresponding to this unknown input.

Firstly, we consider a dynamical system under the influence of disturbances which we can neither control nor measure directly. In order to suppress their effect, we may apply a feedback designed

by, say H_∞ methods (Zhou *et al.*, 1996). If, however, we obtain further information as to how the disturbance affects the system; i.e., if we identify its transfer property, then we can design more effective feedback than the one designed merely for the worst-case disturbance. This is achievable by means of our polynomial matrix ICA method [2].

Our second application is fault detection of a mechanical vibration system. Again we suppose that the system is subject to unknown disturbance, but this time we try to find a parameter change due to fault, only from the output.

This problem is solved by two kinds of methods in this paper. We first apply the ICA algorithm in (Sugimoto and Nitta, 2005) directly. If we can perform identification in real time, this is enough. Real time ICA for dynamical systems is, however, difficult in reality, since it requires a lot of sample data and hence much computational time. To overcome this difficulty, we next propose to combine our polynomial matrix ICA method with conventional FastICA (Hyvärinen and Oja, 1997) and achieve "semi" real-time processing [3].

2. DISTURBANCE SUPPRESSION

2.1 Motivation

Consider the linear discrete-time system

$$\begin{pmatrix} y_1 \\ y_2 \end{pmatrix} = G(z) \begin{pmatrix} d \\ f \end{pmatrix}, G(z) = \begin{pmatrix} g_{11}(z) & g_{12}(z) \\ g_{21}(z) & g_{22}(z) \end{pmatrix}$$

where y_1 and y_2 stand for observed signals, $G(z)$ is a transfer matrix with full normal rank, and d and f are respectively disturbance and control inputs. Assume that both y_1 and y_2 are available for identification as well as feedback, but y_1 only is a signal to be controlled or evaluated (Fig. 1).

To motivate our approach, we start by pointing out the following point: In order to suppress the effect of d to y_1 perfectly, we have the equation

$$\begin{pmatrix} d \\ f \end{pmatrix} = G^{-1} \begin{pmatrix} 0 \\ y_2 \end{pmatrix}, \; G^{-1}(z) = \begin{pmatrix} h_{11} & h_{12} \\ h_{21} & h_{22} \end{pmatrix}.$$

Then, provided that h_{12} is nonzero, there exists $f = (h_{22}/h_{12})d$ such that $y_1 = 0$; i.e., the effect of d to y_1 is perfectly suppressed. Furthermore, this is realized by the linear feedback $f = h_{22}y_2$. This suggests that, if we obtain $G(z)$, then the control performance can be greatly improved.

The above discussion is related to the classical disturbance rejection (Wonham, 1974), but is not always feasible, since this feedback may easily induce instability. It is more practical in general to apply H_∞ methods to this end (Fig. 2).

Usually we design an H_∞ controller according to the policy as in Fig. 3, assuming d in the worst case. This is because, so far, we have been unable to estimate the dynamics corresponding to d. If, in contrast, we use $G(z)$ as in Fig. 4, then we can naturally attain better performance.

We will explain this policy by a numerical example in the next section.

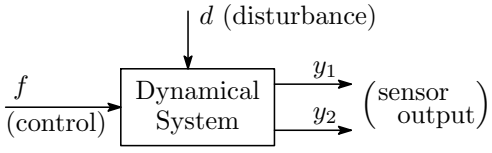

Fig. 1. A disturbance model.

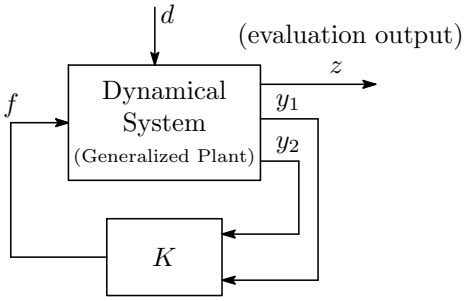

Fig. 2. Disturbance suppression via feedback.

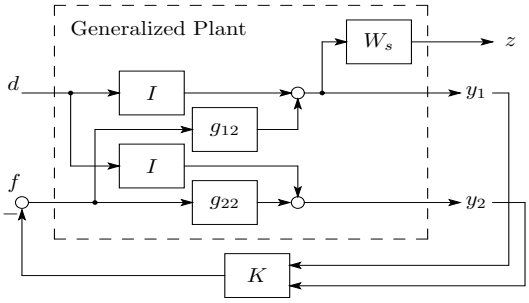

Fig. 3. Ordinary sensitivity optimization problem.

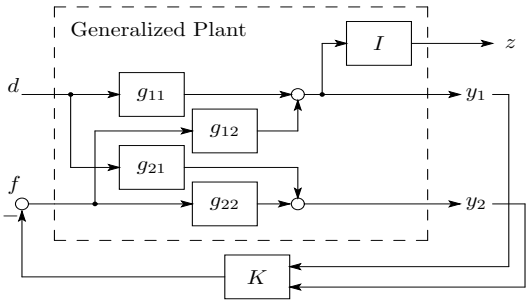

Fig. 4. Proposed feedback control system.

2.2 Numerical Simulation

We adopt the sampling frequency 100 Hz, and use time signal from 0 sec to 2.55 sec, so that

[2] A detailed exposition of this approach can be found in (Nitta and Sugimoto, 2004)

[3] This idea has originally appeared in (Suzuki *et al.*, 2004)

we obtain 256 samples. Let us now consider the transfer matrix in left coprime factorization form $G(z) = D^{-1}(z)N(z)$ such that

$$D(z) = Iz^2 + D_1 z + D_2, \quad N(z) = N_0 z^2$$
$$D_1 = \begin{bmatrix} 0.09 & -0.12 \\ -0.13 & -1.06 \end{bmatrix}, D_2 = \begin{bmatrix} 0.28 & 1.04 \\ 0.08 & 0.58 \end{bmatrix},$$
$$N_0 = \begin{bmatrix} 1.00 & -0.60 \\ 0.20 & 1.00 \end{bmatrix},$$

We have applied input signals (d, f) as in Fig. 5 and observed output signal (y_1, y_2) as in Fig. 6.

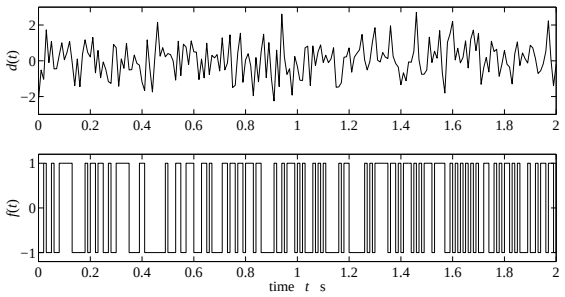

Fig. 5. The waveform of input signals.

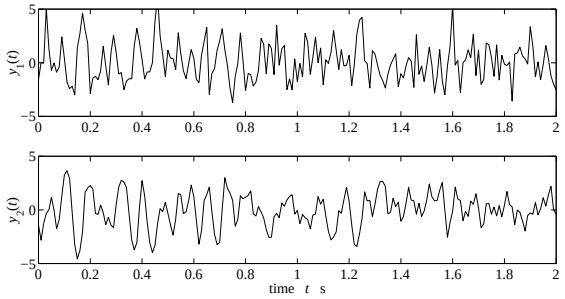

Fig. 6. The output signals.

By means of the polynomial ICA method given by (Sugimoto and Nitta, 2005), we have retrieved the input signal as in Fig. 7, and identified the system parameter as

$$D_1 = \begin{bmatrix} 0.065 & -0.101 \\ -0.155 & -1.029 \end{bmatrix}, D_2 = \begin{bmatrix} 0.256 & 1.021 \\ 0.073 & 0.521 \end{bmatrix},$$
$$N_0 = \begin{bmatrix} 1.000 & -0.536 \\ 0.197 & 1.000 \end{bmatrix},$$

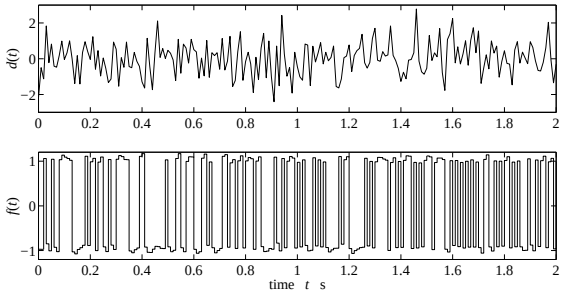

Fig. 7. Estimated input signals.

Although the coefficients are slightly different from the true values, the Bode diagram of the true and the identified systems indicates that they are in good agreement (Fig. 8).

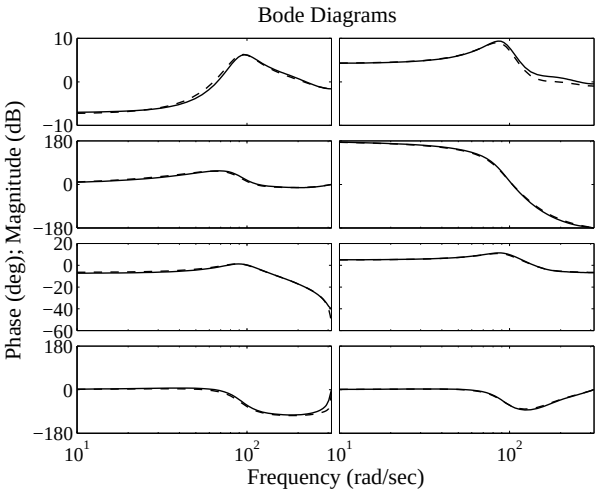

Fig. 8. Bode diagram. (Solid line: estimated value, Dashed: true value)

We have designed H_∞ controller using the generalized plant given in Fig. 3 (conventional method) with the weighting function

$$W_s = \frac{0.001z - 5 \times 10^{-8}}{z - 0.9999}. \tag{1}$$

We have also designed H_∞ controller according to Fig. 4 (proposed approach) with the obtained system parameter. Now Fig. 9 shows the response of the closed-loop systems by these two feedbacks. The upper graph (proposed) indicates that the signals are less than 3×10^{-3}. The effect of the disturbance is drastically suppressed.

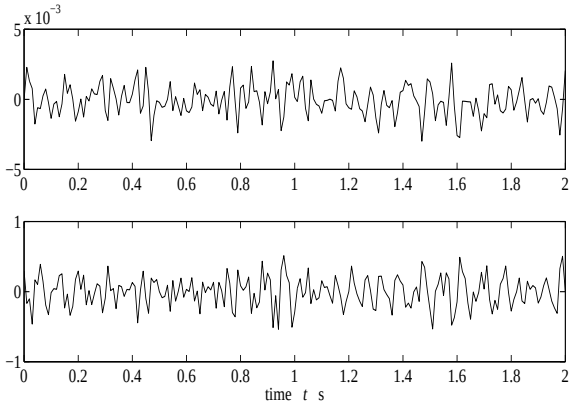

Fig. 9. Response from d to y_1, y_2. (Upper: proposed method, Lower: conventional method. Note that the range of the vertical axis largely differs.)

We have also obtained impulse response of the both closed-loop systems (Fig. 10). Finally, we have computed singular values of the transfer matrices (Fig. 11). The proposed method gives much smaller singular values than other cases.

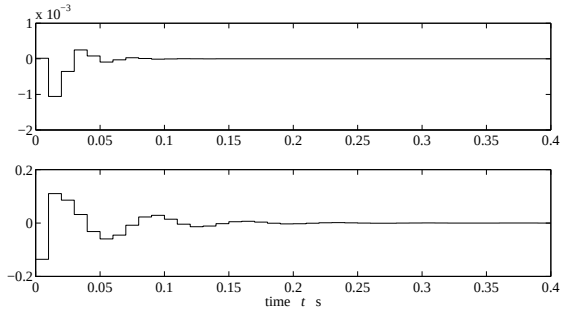

Fig. 10. Impulse response. (Upper: proposed method, Lower: Ordinary method. Note the range of the vertical axis.)

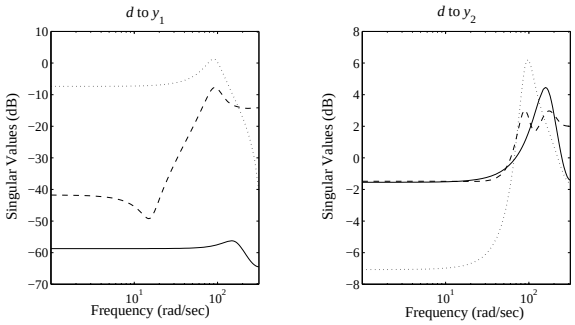

Fig. 11. Singular value plot of d to y_1 and y_2. (Solid line: proposed method, Dashed: conventional, Dotted: control-free)

3. FAULT DETECTION BY OBSERVING OUTPUT ONLY

3.1 Problem Formulation

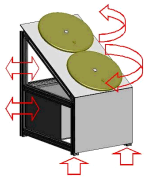

Fig. 12. Roll bending machine.

As a motivation, let us consider a machine (Fig. 12), which is commonly found in manufacturing factories. Such a machine is subject to vibration (i.e., disturbance) from the environment or even from the motion of the machine itself. Even if we can not observe the vibration source directly, we are able to observe the displacement as a result of disturbance. If, further, we detect the change of mechanical structure from these observed signals, and differentiate it from the change of vibration source, then it will be useful since we can find fault by monitering the vibration only.

The authors have performed an experiment to detect a fault of a mechanical system only by observing its vibration. In practice we can measure such vibration (displacement) as a result of disturbance, but can hardly measure the source disturbance (force) in itself. Hence, if a fault of the machine causes a change of the vibration (output), it may appear indistinguishable from the change of the source disturbance (input). However, our method indeed makes it possible to detect the fault only by observing the vibration.

The experimental system is constructed so that it is more vibrant than those in actual manufacturing facilities and we can easily observe the vibration effect (Fig. 13) in the last page. The sensing part consists of displacement sensors and amplifiers (Fig. 14).

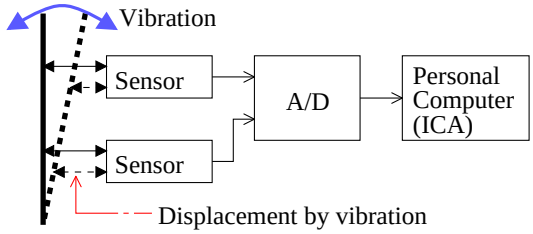

Fig. 14. Signal flow in the experimental system.

3.2 Results of Experiment

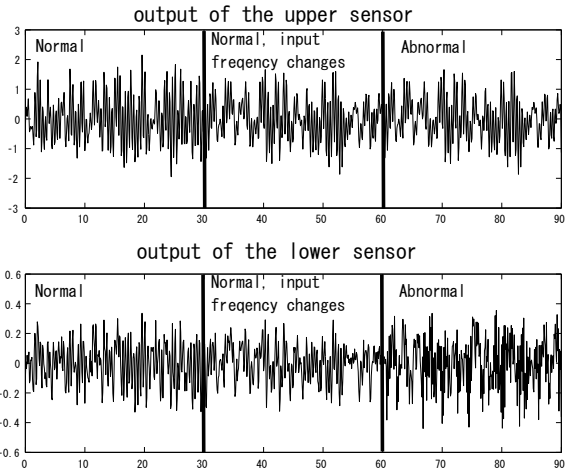

Fig. 15. Observed signals.

Observed signals are shown in Fig. 15. The upper and lower waveforms are those observed by the upper and lower sensors, respectively. The waveforms are in three parts. In the first part the system is in a normal mode. In the second part, it is still in the normal mode, but the frequency of the disturbance signal (motor) changes. In the third part, the system is in an abnormal mode (i.e., fault; see also Fig. 13). In order to avoid error due to transient behavior, these waveforms have been generated individually and combined as data, instead of generating real "fault".

We then compute $G(z)$ by the proposed method. Figs. 16 and 17 show Bode diagram and pole configuration of $G(z)$, respectively.

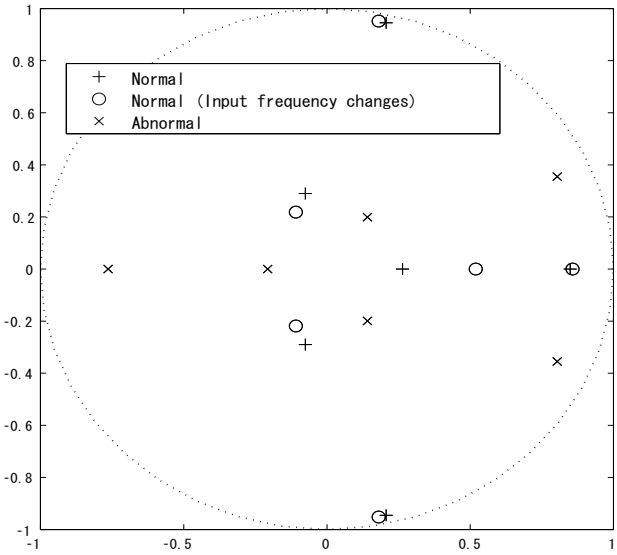

Fig. 17. Poles of the identified systems.

In Fig. 16, some of the shapes are different between "normal" and "normal, input frequency changes," though they should be the same. This is because our assumption made in PART I is not satisfied in this system. Still, the fault can be detected since the peaks are different. Fig. 17 also detects the fault in the sense that the poles shift. Thus we have succeeded in differentiating change in the input and the vibration mode (fault).

From a practical viewpoint, however, the above method is insufficient since real time processing is difficult. By combining FastICA, we have derived a faster algorithm illustrated by Figs. 18, 19, 20.

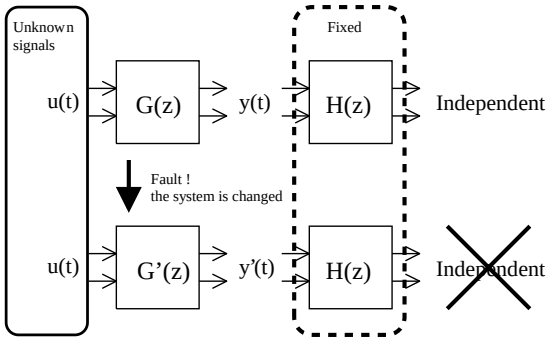

Fig. 18. Block diagram of the proposed algorithm.

4. CONCLUDING REMARKS

In the second application we have succeeded in finding fault in spite that the system does not satisfy the assumption in (Sugimoto and Nitta, 2005). In the authors' opinion, this is because the proposed method can identify partial information of the system even in such a case. This suggests that our method is applicable to a wider class.

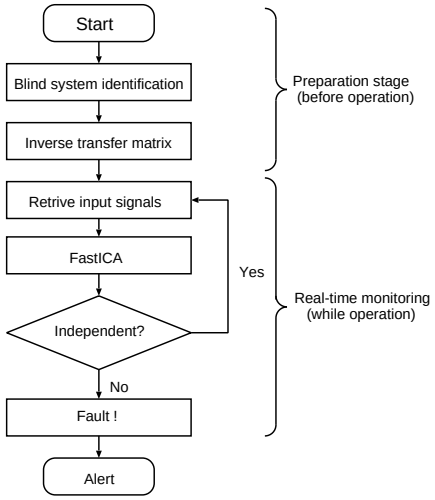

Fig. 19. Flow chart of the proposed algorithm.

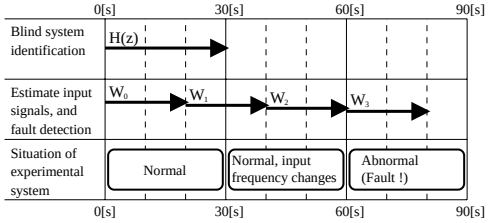

Fig. 20. Time chart of the experiment.

The authors wish to thank reviewers' valuable suggestions, although some of them can not be reflected in the final vesion due to lack of space.

REFERENCES

Hyvärinen, A. and E. Oja (1997). A fast fixed-point algorithm for independent component analysis. *Neural Computation* **9**, 1483–1492.

Ljung, L. (1987). *System Identification — Theory for the User*. Prentie-Hall.

Nitta, M. and K. Sugimoto (2004). A BSD approach to estimation and suppression of disturbance with unknown dynamics by H^∞ feedback. *IFAC Workshop on Adaptation and Learning in Control and Signal Processing, Yokohama, Japan.*

Sugimoto, K. and M. Nitta (2005). Polynomial matrix approach to independent component analysis: (part I) basics. *16th IFAC World Congress, Prague, Czech Republic.*

Suzuki, A., M. Nitta, N. Adachi and K. Sugimoto (2004). Detection of mechanical vibration modes via a blind system identification method. *To be presented at 36th ISCIE Int. Symposimu on Stochastic Systems Theory and Its Applications, Saitama, Japan.*

Wonham, M. (1974). *Linear Multivariable Control*. Springer-Verlag. New York.

Zhou, K., J. Doyle and K. Glover (1996). *Robust and Optimal Control*. Prentice-Hall.

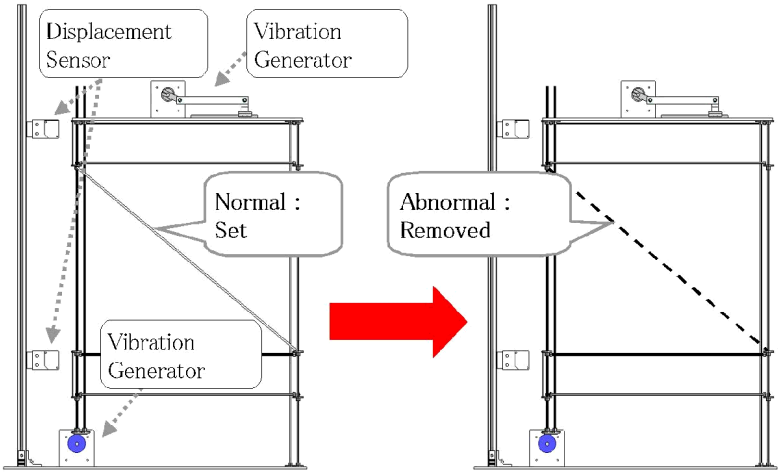

Fig. 13. Appearance of the experimental system.

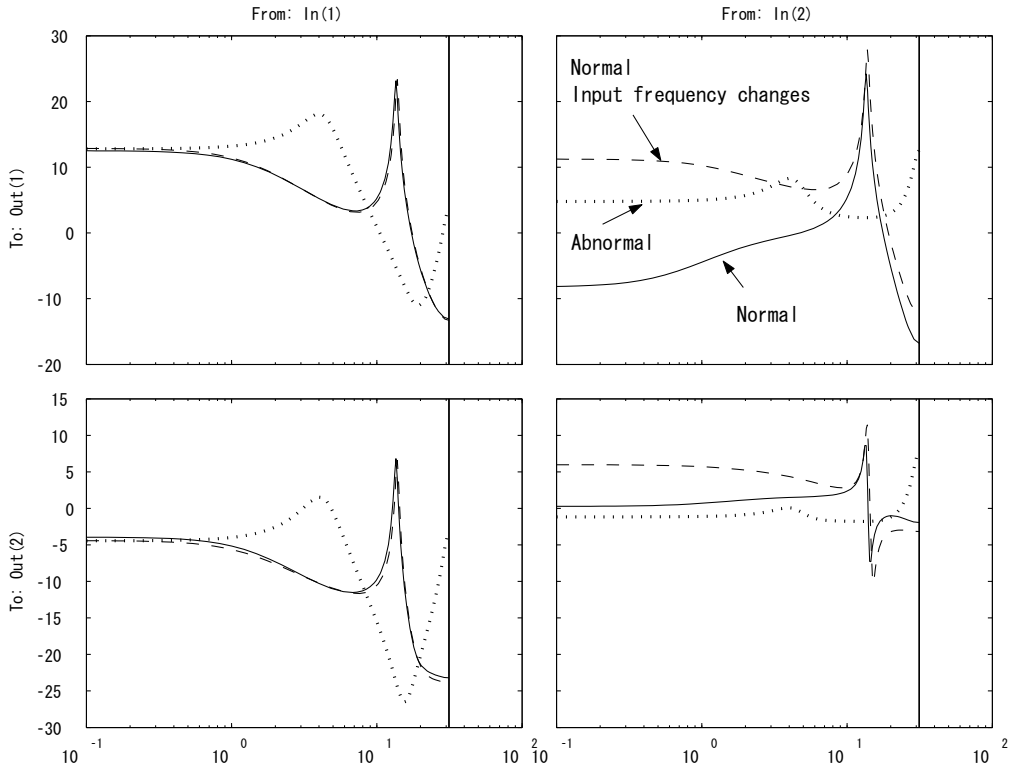

Fig. 16. Bode diagram (magnitude of each entry in 2×2 matrix) of the system identified for three cases.

Table 1. Peak Freqency of bode diagrams and poles.

	Peak frequency (rad/s)	Poles
Normal	13.8	$0.21 \pm 0.95i,\ 0.85,\ -0.08 \pm 0.29i,\ 0.26$
Normal, with disturbance changes	13.8	$0.18 \pm 0.95i,\ 0.86,\ -0.10 \pm 0.22i,\ 0.52$
Abnormal	3.97	$0.8 \pm 0.36i,\ -0.76,\ 0.14 \pm 0.20i,\ -0.21$